DOI: https://doi.org/10.37434/tpwj2025.08.07

IRON-BASED BINDER ALLOY FOR PLASMA TRANSFERRED-ARC SURFACING OF COMPOSITE ALLOYS REINFORCED WITH CAST TUNGSTEN CARBIDES

O.I. Som

Plasma-Master Co., Ltd.
3 Omelian Pritsak Str., 03142, Kyiv, Ukraine

ABSTRACT

Five iron-based industrial alloys with different alloying systems have been studied for the purpose of using them as a binder alloy for plasma-transferred arc surfacing of composite alloys, reinforced with cast spherical tungsten carbides (relite). It is shown that hard and wear-resistant alloys, such as Sormite-1 (PG-S1) and others do not provide an overall increase in the deposited metal wear resistance. Contrarily, they reduce it, as they poorly hold the tungsten carbide grains, which break away and are removed from the friction zone together with the matrix, not contributing to the resistance to wear. Alloys of Kh18N9 type are not suitable, either, as they significantly increase their hardness and thus lower their ductility during surfacing due to additional alloying with carbon and tungsten. The best result was shown by a relatively soft copper-nickel alloy (cast iron) Ni-Resist.

KEYWORDS: plasma transferred-arc surfacing (PTA surfacing), spherical tungsten carbides, binder alloy (matrix), wear resistance, hardness, metal formation

INTRODUCTION

Binder alloy plays a big role in surfacing the wear-resistant composite alloys based on cast tungsten carbides (relite). It should reliably hold the carbide particles from breaking away and provide a high wear resistance of the deposited metal on the whole, particularly under the conditions of impact-abrasive wear. Moreover, it should ensure good formation of the deposited metal and resistance to cracking in welding.

In practice low-melting self-fluxing nickel-based alloys of Ni–Si–B or Ni–Cr–Si–B–C systems of different hardness are widely used as binder alloy for plasma transferred arc (PTA) surfacing of composite alloys reinforced with tungsten carbides [1, 2, 12].

A disadvantage of application of such alloys, particularly in high-productivity surfacing (>3 kg/h), is spatter deposition on the plasma torch edge, which over time clogs the powder feed channel in long-term operation, and, consequently, disrupts the technological process of surfacing. During application of plasma torches with inner powder feed [3] the surfacing process disruption occurs even faster, because of metal drops appearing at the outlet of the focusing nozzle.

Proceeding from that, iron-based alloys are attractive in terms of increasing the stability of the surfacing process. They have higher melting temperature and are less prone to drops forming at the plasma torch outlet during surfacing. In addition, they are much less expensive than the nickel alloys. Attempts to use iron-based alloys as a binder alloy were made before [4, 5], but they are not of a systemic nature, and do not provide replies or recommendations as to alloy selection.

OBJECTIVE OF THE WORK

The objective of this work is searching for an iron-based commercial alloy for using it as a binder during PTA surfacing of composite alloys based on tungsten carbides.

Selection criteria are as follows: formation of the deposited metal; crack resistance of the deposited composite metal; surfacing process stability; wear resistance under the conditions of abrasive wear; strength of deposited metal adhesion to the base.

INVESTIGATION MATERIALS

The following industrial alloys, which in the author's opinion can be used as the binder alloy, were selected for investigations (Table 1). These alloys are produced by various foreign manufacturers in the form of powders suitable for PTA surfacing. Powders of 63–160 μm fraction were used in the experiments.

To compare the service properties of the deposited metal, we also used in the experiments the known surfacing composite powder Durmat 61-PTA produced by DURUM Verschleißschutz GmbH (Germany), which is a mixture of powders of Durmat 59-PTA grade (nickel-based alloy of Ni–Si–B system of 50 *HRC* hardness) and crushed tungsten carbide in the proportion of 40:60 wt.%, respectively.

The selected alloys differ significantly by chemical composition, deposited metal type, hardness and wear

Copyright © The Author(s)

Table 1. Chemical composition of iron-based alloys used in the experiments as binder alloy

Binder alloy type (powder grade)	Chemical element composition, wt.%								Hardness, *HRC*
	C	Mn	Si	Cr	Ni	V	Mo	Cu	
1. 08Kh18N9 (PR-Kh18N9)	0.08	0.7	0.5	18.0	9.5	–	–	–	140 *HB*
2. 270N15D7Kh3CS2 (PR-ChN15D7)	2.7	0.8	2.1	2.8	14.8	–	–	6.5	26
3. 220Kh18F7N3M2 (PMalloy 21)	2.2	0.8	0.7	17.8	2.8	7.1	2.4	–	46
4. 300F11Kh6NM (Plasweld™FerroV10)	3.0	0.9	0.8	6.0	0.6	10.8	1.4	–	60
5. 300Kh30N4S2 (PG-S1)	3.0	1.2	3.2	29.8	4.0	–	–	–	54

resistance. Such a wide range of the alloys allows for better assessment of the influence of matrix type on the welding-technological and service properties of the composite deposited metal.

BRIEF CHARACTERISTICS OF THE ALLOYS

Alloy No. 1 is the classic (18–9) chromium-nickel steel of austenitic class. It is characterized by a high corrosion resistance and ductility, which is highly important under the conditions of abrasive wear with impacts. Application of such steel as the binder alloy is described in work [5].

Alloy No. 2 is the copper-nickel cast iron of austenitic class, known under the Ni-resist brand name [6]. It also has high corrosion resistance and ductility. In addition, it is non-magnetic and has high antifriction properties. The high carbon content ensures its good welding technological properties.

Alloys Nos 3 and 4 belong to the class of wear-resistant high-vanadium cast irons, the valuable properties of which are a fine-grained structure and increased impact toughness [7]. The main wear-resistant phase in them is primary vanadium carbides VC. We selected two compositions for the experiments, which differ by matrix type, hardness and wear resistance.

Alloy No. 3 has an austenitic-martensitic matrix with 44–46 *HRC* hardness, which ensures that it optimally combines high wear resistance with ductility required for resistance to impact loads and to cracking during surfacing [8].

Alloy No. 4 has a martensitic matrix with low austenite content (6–8 %). Its hardness after PTA surfacing is equal to 60–62 *HRC*. Compared to alloy No. 3, the deposited metal has more carbide phase, due to a higher alloying with vanadium and carbon.

Alloy No. 5 is a high-chromium cast iron of hypereutectic type, known as Sormite 1, which is characterized by a high wear-resistance under the conditions of abrasive wear. The structure of metal deposited with it consists of coarse chromium carbides of $Cr_{23}C_6$ type, carbide eutectics and residual austenite [9].

Used as the reinforcing wear-resistant material was powder of spherical tungsten carbide of 100–200 μm fraction, produced by Resurse-1 Ltd., Ukraine [10].

Deposition was performed on ground plates from steel 20 of 120×120×25 mm size, using equipment of Plasma-Master LTD Company with a plasma torch of RR-6-03 model (Figure 1).

The matrix and reinforcing powders were fed separately from two feeders in the proportion of 40:60 wt.% to avoid their separation and to maintain this proportion constant during the surfacing process. The powders were supplied to the weld pool as a mixture, formed by merging of the two flows directly at the inlet to the plasma torch.

Several surfacing variants were realized in the experiments. Both single and double beads were deposited with an overlap (Figure 2). Surfacing

Figure 1. Plasma transferred-arc surfacing unit with two powder feeders and RR-6-03 plasma torch

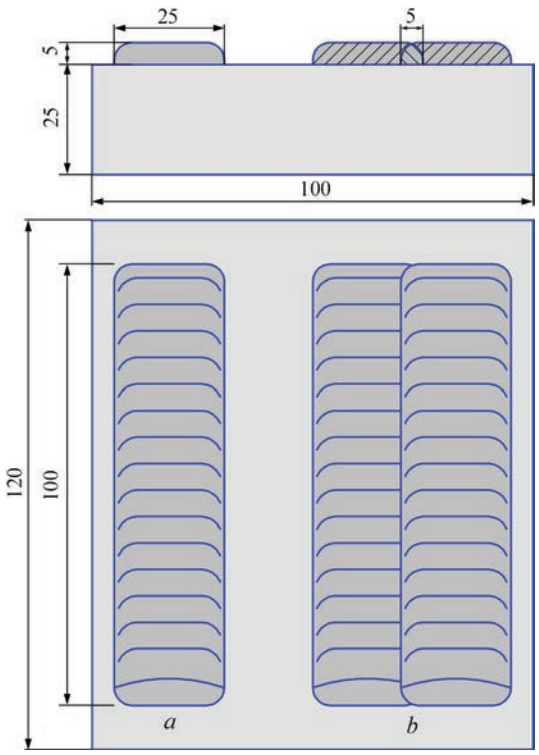

Figure 2. Schematic of surfacing the plates to study the formation and crack resistance of the deposited metal: *a* — single bead; *b* — double bead with an overlap

was performed without the sample preheating, with preheating to 300 °C and using an underlayer from chromium-nickel austenitic steel 08Kh18N9. The preheating and the underlayer were used as methods to prevent cracks in the deposited metal. Samples of 16×16×6 mm size (Figure 3, *a*) for testing the alloys for wear resistance in NK machine (stationary ring) [11] and samples of 50×16×8 mm size for surfaced metal testing for delamination during bending (Figure 3, *b*) were cut out of the surfaced plates by spark method. The upper part of the deposited layer in both the cases was ground to the level, at which the tungsten carbide particles were relatively uniformly distributed over the cross-section. The same samples were used for metallographic studies.

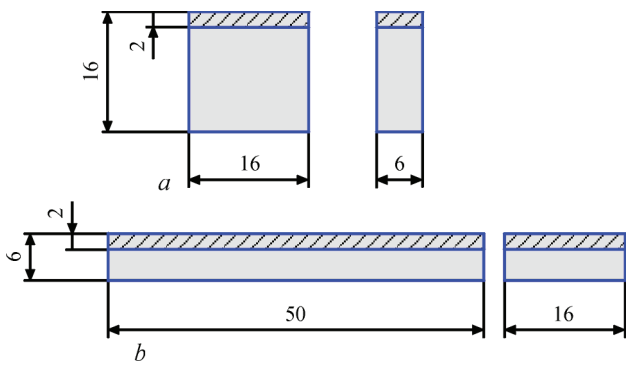

Figure 3. Samples for studying the deposited metal wear resistance in NK machine (*a*) and its delamination from the base during bending (*b*)

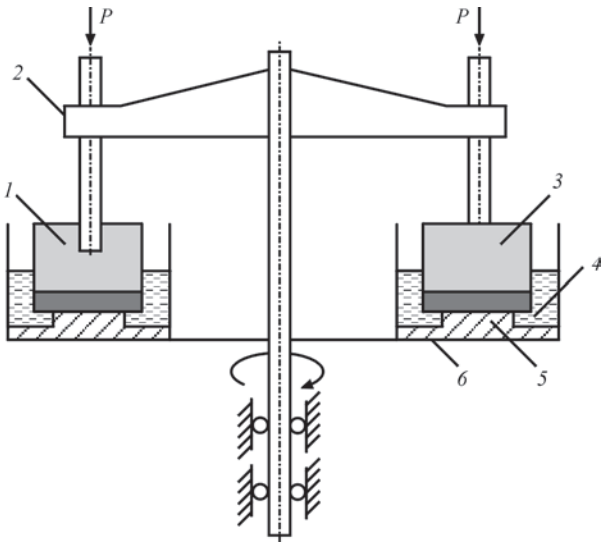

Figure 4. Schematic of wear resistance testing of surfaced samples in NK machine: *1* — test sample; *2* — rotating cross-piece; *3* — standard; *4* — abrasive with water; *5* — copper ring; *6* — bed plate

Quality of the deposited metal formation was assessed visually, and presence of cracks — visually and using dye penetrant flaw detection.

Schematic of wear resistance testing of the surfaced samples is shown in Figure 4.

Testing conditions were as follows: load on the sample — 3 kg, friction path — 700 m, sliding (friction) speed — 6 m/s, abrasive medium — wet river quartz sand.

The standard was annealed steel 45, which was used to control the wear conditions. The friction path length was selected from the condition of producing a noticeable wear of samples. Wear resistance was assessed by the loss of sample weight, using scales with up to 0.001 g precision.

Testing the samples for deposited metal delamination from the base was performed under static loading in the press by the schematic shown in Figure 5. Loading was applied from the base metal side. Bend angle was 150°.

Deposited metal microstructure was studied using Neophot-21 photomicroscope, and the microhardness was measured in Leco M400 Instrument.

ANALYSIS OF EXPERIMENTAL RESULTS. BEAD FORMATION

All the considered compositions without exception provide very good formation of the deposited metal, both during deposition of single beads and double

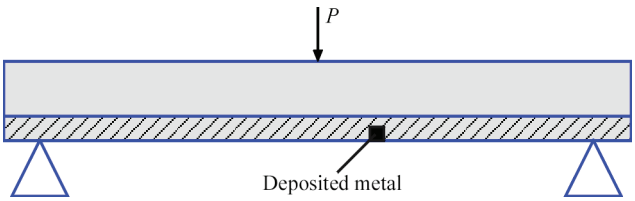

Figure 5. Schematic of testing samples for deposited metal delamination from the base

beads with an overlap. The beads are even and clean, without any traces of slag. In the points of bead overlapping in two-pass surfacing the metal is also clean. Base metal penetration is practically absent, which confirms the optimal balance of the surfacing parameters. Figure 6 shows as an example the appearance of the beads deposited using a composite alloy with binder No. 2 (270N15D7Kh3S2).

CRACKS IN THE DEPOSITED METAL

Visual examination and dye penetrant testing showed that cracks are present in some of the deposited beads. In case of deposition of individual beads without preheating cracks were observed in compositions Nos 1 and 5 (Table 2). They were located across the beads with minimal opening.

For variant No. 1 this is unexpected to some extent, considering the soft austenitic matrix. As shown by metallographic studies, however, it is soft only in surfacing without tungsten carbides (Table 2). In the presence of tungsten carbides its hardness HV_{01} is significantly increased from 150 to 600. It occurs due to additional alloying of the matrix with carbon and tungsten as a result of partial dissolution of tungsten carbide grains during surfacing, which is confirmed by X-ray microprobe analysis. With increase of the matrix hardness its ductility decreases naturally, leading to appearance of cracks in the deposited metal. During surfacing with preheating, no cracks were further observed in composition No. 1, and in composition No. 5 their number was greatly reduced. They disappeared completely in case of surfacing with preheating on the underlayer (Table 2).

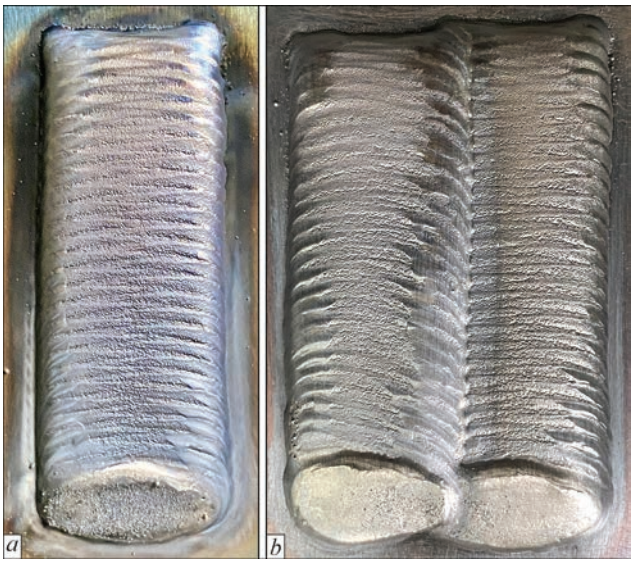

Figure 6. Appearance of beads deposited using a composite alloy with binder No. 2 (270N15D7Kh3S2): *a* — single bead; *b* — double bead with an overlap

Crack situation deteriorates considerably during deposition of beads with an overlap without sample preheating. Such a variant is observed during continuous surfacing of large surfaces (for instance, armor plates) and in deposition of closed circular beads. Cracks are observed both in the first and in the next beads. Their nature is different in different alloys. In compositions Nos 1 and 5 (Table 2) they look like a net (Figure 7, *a*), and in compositions Nos 3, 4 and 6 they look like isolated cracks, located approximately normal to the solidification layers. Only one crack was revealed in composition No. 2 (Figure 7, *b*).

Table 2. Results of investigation of cracking resistance of experimental composite alloys during surfacing

Composition	Number of cracks per 100 mm of the deposited bead length						Average microhardness of the matrix, HV_{01}	
	Single bead deposition			Deposition of two beads with overlap				
	Without preheating	With preheating 300 °C	With preheating on underlayer 300 °C	Without preheating	With preheating 300 °C	With preheating on underlayer 300 °C	Pure (without tungsten carbides)	With tungsten carbides
1. 08Kh18N9 + tungsten carbides	1	0	0	Network of cracks	1	0	150	600
2. 270N15D7Kh3S2 + tungsten carbides	0	0	0	1	0	0	270	400
3. 220Kh18F7N3M2 + tungsten carbides	0	0	0	2	1	0	440	460
4. 300F11Kh6NM + tungsten carbides	0	0	0	4	1	0	690	720
5. 300Kh30N4S2 + tungsten carbides	3	1	0	Network of cracks	2	1	580	610
6. Ni–Si–B + tungsten carbides	0	0	0	2	1	0	–	600

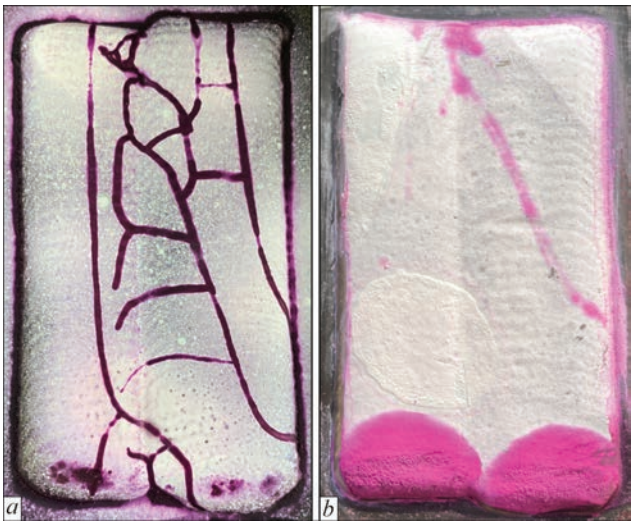

Figure 7. Cracks in deposited compositions: *a* — 08Kh18N9 + tungsten carbides; *b* — 220Kh18F7N3M2 + tungsten carbides

The cause for appearance of additional cracks is the thermal impact on the previous bead, having a high level of internal stresses, as well as higher rigidity of the joined beads.

Preheating noticeably decreases the number of cracks in the deposited metal, and presence of an underlayer from austenitic chromium-nickel steel even more promotes their reduction (Table 2). Cracking cannot be avoided only in deposition of composition No. 5 with binding alloy 300Kh30N4S2 (Sormite 1).

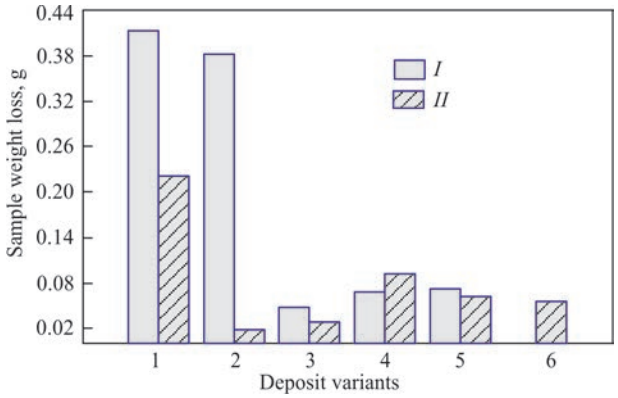

Figure 8. Diagram of wear resistance of the deposited metal variants tested in NK machine: *I* — pure binder alloy; *II* — composite alloy with tungsten carbides

DEPOSITED METAL WEAR RESISTANCE

As was mentioned above, the wear resistance of the surfaced samples was tested in the NK laboratory machine. The results are given in Table 3 and in Figure 8.

For better understanding of the matrix influence on the composite alloy wear resistance, an investigation of wear resistance of the matrices proper without the tungsten carbides was conduced separately. The results are given in the same work.

From the given results it is clearly seen that the composition in which a relatively soft copper-nickel austenitic cast iron Ni-resist (No. 2) is used as the binder alloy has the highest wear resistance in the

Table 3. Results of wear resistance testing of the deposited alloys

Type of binder alloy	Loss of sample weight, g		Binder alloy hardness, *HRC*
	Pure binder alloy	Composite alloy (binder alloy + tungsten carbides)	
1. 08Kh18N9	0.412	0.221	140 *HB*
2. 270N15D7Kh3S2	0.382	0.018	26
3. 220Kh18F7N3M2	0.048	0.028	46
4. 300F11Kh6NM	0.068	0.092	60
5. 300Kh30N4S2	0.072	0.062	54
6. Ni–Si–B–C	–	0.055	50

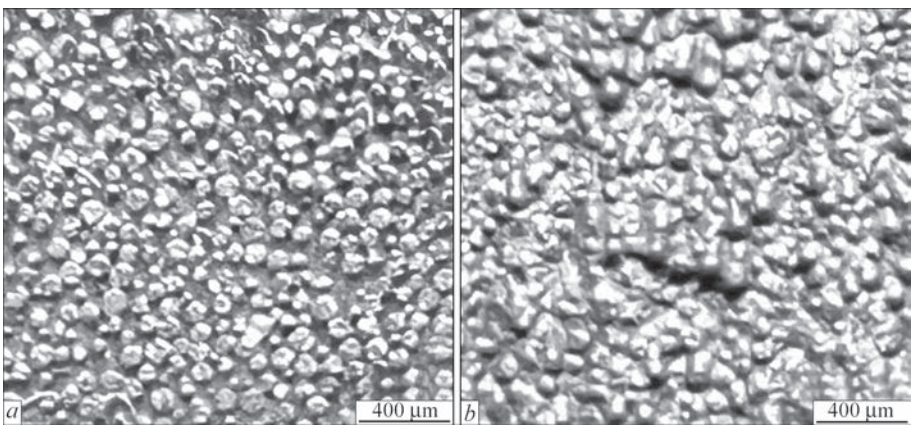

Figure 9. Texture of friction surfaces of the deposited composite alloys after testing: *a* — 270N15D7Kh3S2 (No. 2) + tungsten carbides; *b* — 300F11Kh6NM (No. 4) + tungsten carbides

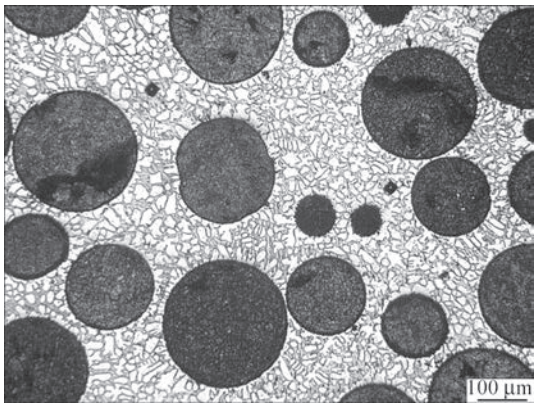

Figure 10. Deposited metal microstructure

abrasive wear conditions. Compared to pure alloy, the deposited metal wear resistance when adding tungsten carbides to it rose more than 20 times. This is due to the fact that this alloy holds the tungsten carbide grains in the matrix very well, forcing them to take on all the wear energy. Tungsten carbide grains on the friction surface wear relatively evenly, maintaining a flat round shape (Figure 9).

Figure 10 is the microstructure of this composite deposited metal, which clearly shows the shape and distribution of the spherical tungsten carbide grains in the matrix. As we can see, they are well preserved without any noticeable melting or dissolution. The matrix proper has a fine-grained eutectic structure, consisting of an iron-based solid solution and carbides of cementite type $(Fe, Cr)_3C$. No free graphite is visible.

A somewhat worse result was demonstrated by the variant with the austenitic-martensitic matrix 220Kh18F7N3M2 (No. 3) (Figure 8). At the same time, it is worth mentioning that the wear resistance of this composition with tungsten carbides, compared to the pure alloy, increased only slightly, just 1.7 times. The alloy proper without the tungsten carbides resists wear well, due to the presence in its structure of up to 70 % of metastable alloyed austenite and a large quantity of primary vanadium carbides VC [8]. During friction such austenite transforms into deformation martensite, while absorbing the fracture energy.

The hope for a high wear resistance of the composition with binder alloy 300F11Kh6NM (No. 4) was not

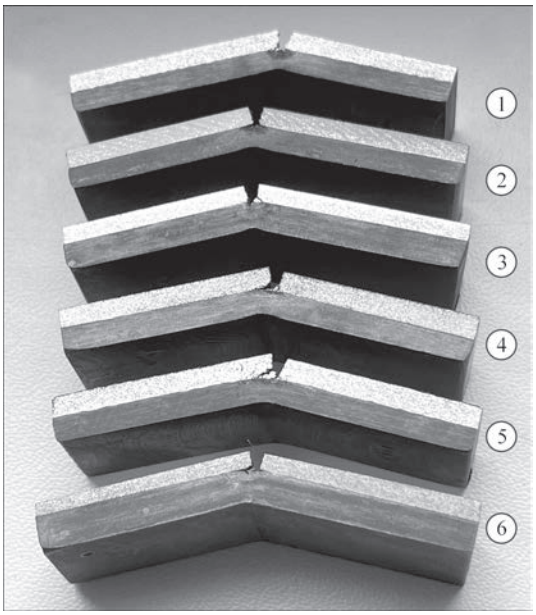

Figure 11. Deposited samples after testing for delamination from the base during bending. Sample numeration is given according to Table 2

justified. Despite the high hardness of the binder alloy (60 *HRC*) and large quantity of vanadium carbides in it, its wear resistance is generally not high (Figure 8). Paradoxically, it is lower than that of the pure alloy. The explanation of that may be that the hard martensitic matrix does not hold the carbide grains well, which under such conditions are just torn out and are carried out of the friction zone together with the matrix and thus the wear resistance is reduced. This is clearly visible in the texture of the friction surface (Figure 9). Since the density of tungsten carbides is much higher than that of the matrix, its influence on the total loss of sample weight is more noticeable in this case.

Wear resistance is not noticeably increased in composition No. 5 based on 300Kh30NH4S2 (Sormite 1), either, by just 12–15 %. Here also the strength of tungsten carbide grains fixing to the matrix plays a role.

Composition No. 6 (Durmat 61-PTA) based on nickel alloy of Ni–Si–B system showed a good result (Figure 8), although it is noticeably inferior to compositions Nos 2 and 3. This leads to the conclusion that the latter can be a good replacement for it.

Figure 12. Examples of effective application of PTA surfacing of a composite alloy with 270N15D7Kh3S2 binder alloy: *a* — tangential cutter; *b* — calibrator; *c* — leveling valve of blast furnace

DEPOSITED METAL DELAMINATION

Results of testing the deposited samples for delamination are shown in Figure 11. As we can see, the deposited layer fracture is brittle in all the compositions, without bending. All the samples have one crack each in the site of load application. No delamination from the base metal was noted. This gives grounds to state that the deposited metal adhesion to the base in all the variants of the composition is strong, and under the real conditions presence of cracks in it should not have any noticeable influence on its total performance.

Thus, analysis of laboratory studies showed that there are iron-based alloys, which cannot be used as the binder alloys for PTA surfacing with composite alloys based on tungsten carbides, and there are alloys which are highly promising for this purpose, for instance Nos 2 and 3 (Table 1).

Alloy No. 2 (270N15D7Kh3S2) was selected for industrial trials, which showed the best wear resistance and good formation of the deposited metal.

Figure 12 shows examples of effective application of PTA surfacing of the composite alloy using this binder alloy.

CONCLUSIONS

1. Iron-based alloy can be used with success as binder alloy for PTA surfacing of tungsten carbides. However, one should not use alloys, which, in combination with tungsten carbides significantly increase their hardness during surfacing, thus lowering the ductility. The high hardness impairs the fixation of the tungsten carbide grains, they are torn off, as a result of which a high wear resistance of the deposited metal is not achieved.

2. Wear-resistant alloys with a high hardness when applied as the binder alloy do not provide any noticeable increase in the deposited metal wear resistance.

3. The relatively soft copper-nickel austenitic cast iron Ni-resist yielded the best result as the binder alloy. It provides excellent formation of the deposited metal, high wear resistance, and it is not too prone to cracking. This alloy can be recommended for wide application as a binder alloy for PTA surfacing based on tungsten carbides.

REFERENCES

1. Harper, D., Gill, M., Hart, K.W.D., Anderson, M. (2002) Plasma transferred arc overlays reduce operating costs in oil sand processing. In: *Proc. of Inter. Spray Conf. on YTSC 2002, Essen, Germany, May*, 278–283.
2. Bouaifi, B., Reichmann, B. (1998) New areas of application through the development of the high-productivity plasma-arc powder surfacing process. *Welding and Cutting*, 50(**12**), 236e–237e.
3. Som, A.I. (1999) New plasmatrons for plasma-powder surfacing. *Avtomaticheskaya Svarka,* **7**, 44–48.
4. Som, A.I. (2004) Plasma-powder surfacing of composite alloys based on cast tungsten carbides. *The Paton Welding J.,* **10**, 43–47.
5. Renyue Yuan, Xuewei Bai, Haozhe Li et al. (2021) Effect of WC content on microstructure, hardness, and wear properties of plasma cladded Fe–Cr–C–WC coating. *Materials Research Express,* 8(**6**), 066302. DOI: https://doi.org/10.1088/2053-1591/ac0b79
6. Fischer, J. (2022) Properties and applications of Ni-resist and ductile Ni-resist alloys. 2nd Edition. www: https://nickelinstitute.org/media/8da7c3cd6014c9b/11018_properties_and_applications_of_ni-resist_alloys.pdf
7. Pereplyotchikov, E.F., Ryabtsev, I.A., Gordan, G.M. (2003) High-vanadium alloys for plasma-powder cladding of tools. *The Paton Welding J.*, **3**, 14–17.
8. Som, A.I. (2016) Iron-based alloy for plasma-powder surfacing of screw conveyors of extruders and injection molding machines. *The Paton Welding J.,* **7**, 21–25. DOI: https://doi.org/10.15407/tpwj2016.07.04)
9. Frumin, I.I. (1977) Modern types of clad metal and their classification. In: *Theoretical and technological fundamentals of cladding. Clad metal.* Kyiv, Naukova Dumka, 3–17.
10. Zhudra, A.P. (2014) Tungsten carbide based cladding materials. *The Paton Welding J.,* **6–7**, 66–71. DOI: https://doi.org/10.15407/tpwj2014.06.14
11. Yuzvenko, Yu.A., Gavrish, V.A., Marienko, V.Yu. (1979) Laboratory units for assessment of wear resistance of clad metal. In: *Theoretical and technological fundamentals of cladding. Properties and tests of clad metal.* Kyiv, PWI, 23-27.
12. Augustine Nana Sekyi Appiah, Oktawian Bialas, Artur Czupryński, Marcin Adamiak (2022) Powder plasma transferred arc welding of Ni–Si–B+60 wt% WC and Ni–Cr–Si–B+45 wt% WC for surface cladding of structural steel. *Materials,* 15(1**4)**, 4956. DOI: https://doi.org/10.3390/ma15144956

ORCID

O.I. Som: 0009-0009-4152-4832

CORRESPONDING AUTHOR

O.I. Som
Plasma-Master Co., Ltd.
3 Omelian Pritsak Str., 03142, Kyiv, Ukraine
E-mail: info@plasma-master.com

SUGGESTED CITATION

O.I. Som (2025) Iron-based binder alloy for plasma transferred-arc surfacing of composite alloys reinforced with cast tungsten carbides.
The Paton Welding J., **8**, 68–74.
DOI: https://doi.org/10.37434/tpwj2025.08.07

JOURNAL HOME PAGE

https://patonpublishinghouse.com/eng/journals/tpwj

Received: 10.04.2025
Received in revised form: 26.06.2025
Accepted: 04.08.2025